Supporting Information for

Stability and effect of PbS nanoinclusions in thermoelectric PbTe

*Christian Moeslund Zeuthen,[a] Lasse Rabøl Jørgensen,[a] Lise Joost Støckler,[a] Martin Roelsgaard,[a] Ann-Christin Dippel[b] and Bo Brummerstedt Iversen[a]**

[a]Center for Materials Crystallography, Department of Chemistry and iNANO, Aarhus University, DK-8000 Aarhus C, Denmark

[b]Deutsches Eleketronen-Synchrotron DESY, 22607 Hamburg, Germany

*Corresponding author: bo@chem.au.dk

Particle size calculation

The crystallite size, D, can be calculated using the Scherrer equation, $D = \frac{K\lambda}{\beta_{size}cos(\theta)}$, where *K* is a shape factor (Set to 1), λ is the wavelength of the incoming X-rays, β_{size} is the profile broadening due to size effects and θ is the peak position. Any instrumental broadening is subtracted by refining a LaB_6 standard and using an IRF in *FullProf*.

The following deduction follows both Thompson *et al.*[1] and the *FullProf* manual closely. In this study, the Thompson-Cox-Hastings function is used to represent the profile parameters and the Full-width-at-half-maximum (FWHM) of the *k*'th reflection (H_k) can be calculated using

$$H_k = \left(H_g^5 + AH_g^4H_L + BH_g^3H_L^2 + CH_g^2H_L^3 + DH_gH_L^4 + H_L^5\right)^{1/5},$$

where A, B, C and D are constants, which can be found in the original article, H_g (H_L) is the FWHM of the Gaussian (Lorentzian) component given as

$$H_G = \left(U\tan^2\theta + V\tan\theta + W + Z\cos^{-2}\theta\right)^{1/2} \text{ and}$$

$$H_L = X\tan\theta + Y\cos^{-1}\theta \quad (1)$$

The size of particles is known to broaden peak with a $\cos^{-1}\theta$ dependency and therefore the broadening due to size effects can be determined as

$$H_{S,k} = \left(Z^5 + AZ^4Y + BZ^3Y^2 + CZ^2Y^3 + DZY^4 + Y^5\right)^{1/5}.$$

In this experiment, it was not necessary to use the Gaussian profile to obtain a satisfactory fit and therefore this reduces to

$$H_{S,k} = Y.$$

The profile broadening, β_{pV}, is then calculated from the pseudo-Voigt function, where *Y* is transformed to radians (as FullProf uses degrees)

$$\beta_{pV(size)} = \frac{\pi Y}{2}\left(\frac{\pi}{180}\right)\cos^{-1}\theta.$$

This broadening must be the same as the broadening, β_{size}, from the Scherrer equation, so

$$\frac{K\lambda}{\cos\theta D} = \frac{Y\pi^2}{360\cos\theta}$$

And

$$D = \frac{K360\lambda}{Y\pi^2}.$$

In this study, the most important part is not the absolute values of the crystallite size, but instead the evolution of the size. Therefore K is set to unity, whereas it truly is dependent on the shape of the crystallites. Additionally, as the PbS phase peaks are quite weak in the beginning of the experiment, the absolute size should not be trusted during this period. Using only the Lorentzian contribution should not be a large issue, as size effects are known to be mostly (or entirely) Lorentzian. Strain in the sample should in theory be completely separate from size effects, but in reality, they can be correlated to a certain degree. This also introduces uncertainty as to the absolute size of the crystallite. In contrast, the relative evolution of the crystallite size is more certain, as K and instrumental variables should be constant throughout the experiment and therefore not affect the evolution, only the absolute sizes.

In some experiments, a decreasing crystallite size is observed during heating, which we expect to be an experimental artifact. In these experiments, we heat the sample from room temperature to 475 °C over a period of 15 minutes, which amounts to a heating rate of 30 °C/min or 0.5 °C/sec. During the five seconds exposure time of each dataset, the temperature of the sample therefore increases with approximately 2.5 °C, which will cause the unit cell to expand according to:

$$\Delta L = L(T)\alpha_L(T)\Delta T$$

Where $L(T)$ is the length of the unit cell and $\alpha_L(T)$ is the linear thermal expansion coefficient at temperature T. From Figure 1c in the manuscript, it is observed that the unit cell expands during heating, and a study by Sadovnikov *et al.*[5] furthermore reports a slightly increasing linear thermal expansion coefficient with temperature. As such, the unit cell will expand more in absolute terms during acquisition of diffraction data at higher temperatures.

Expansion of the unit cell during data acquisition causes Bragg's law to be fulfilled at a span of 2θ values for all diffraction peaks. In a Rietveld refinement, this effect would normally be described as microscopic strain, with an angular dependency of tan(2θ), but since we do not include microscopic strain in our Rietveld model, the effect will instead be absorbed by the Scherrer broadening parameter, which has an angular dependency of 1/cos(2θ). Hence, the result will be a decrease of the apparent crystallite size in region I of the experiment.

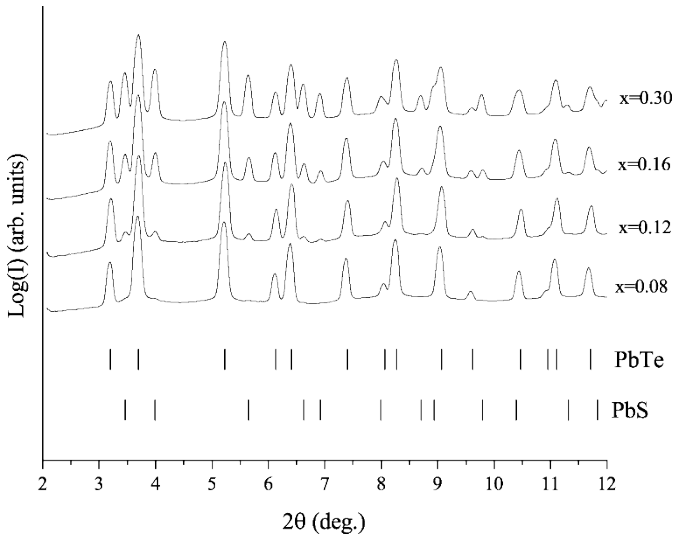

Figure SI 1: Diffractograms of all samples, with x signifying the amount of PbS, investigated by ATHOS before exposure to heat or current. Lines showing expected peak positions can be seen in the area below the diffractograms. It is clear that the PbS peaks are becoming increasingly pronounced with increasing x and that they are barely visible in x=0.08. The intensity is shown on the log-scale to enhance the contrast between the PbS (ICSD #38293) and PbTe (ICSD #63098) phases.

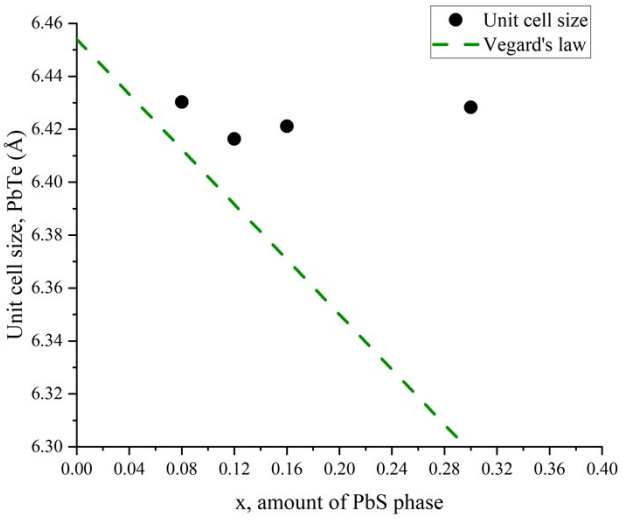

Figure SI 2: Unit cell parameter of PbTe matrix for samples with varying x. The dashed line is value from Vegard's law calculated using ICSD data for pure PbTe and PbS. The samples show similar behavior as seen by Girard et. al.[2]

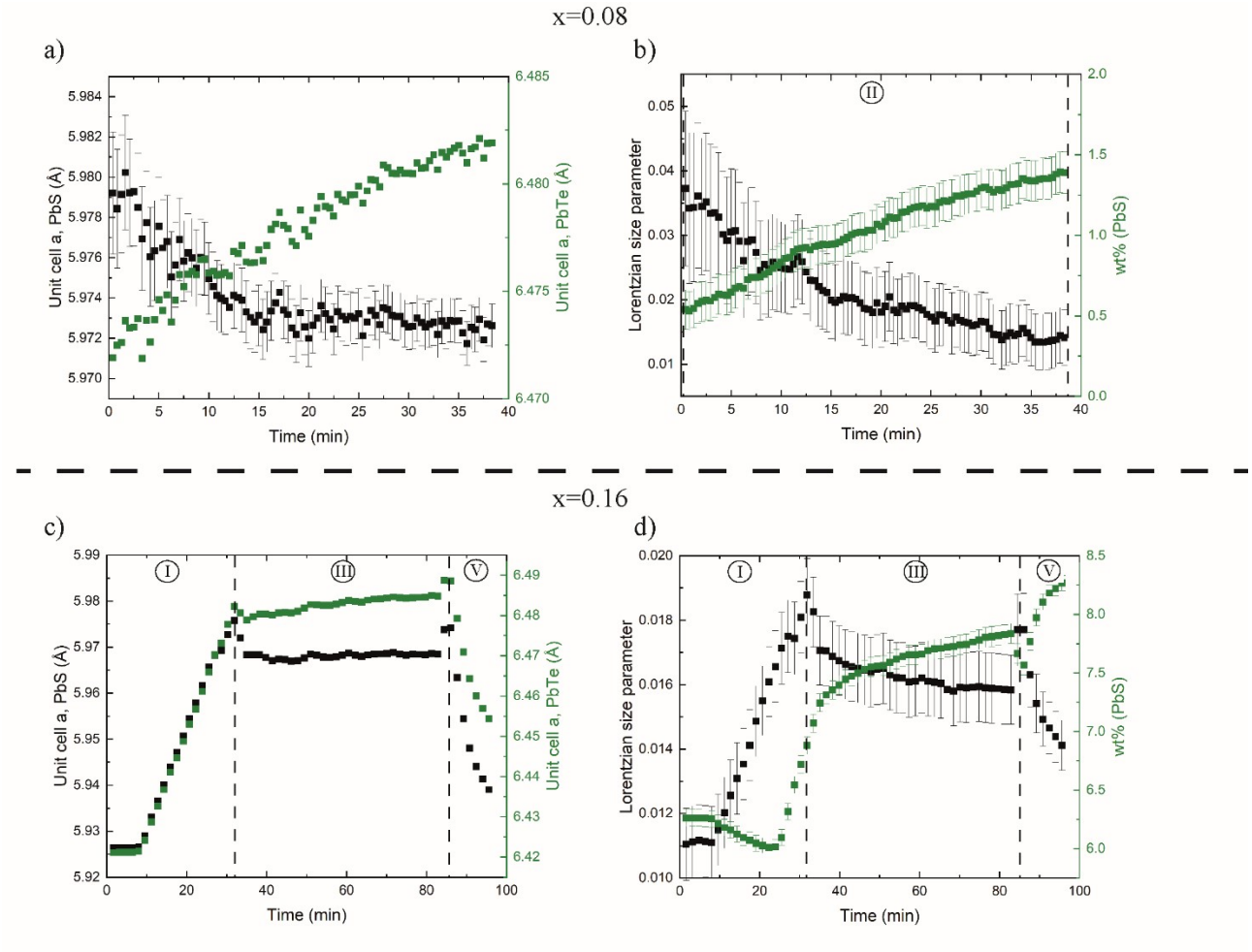

Figure SI 3: Time-resolved Rietveld refinement parameters of samples $Pb_{0.98}Te_{0.92}S_{0.08}Na_{0.02}$ (Top) containing only one isotherm region (II) and $Pb_{0.98}Te_{0.84}S_{0.16}Na_{0.02}$ (Bottom) containing heating (I), isotherm + current (III) and cooling (V). a) & c) Unit cell parameter of PbTe matrix (black) and PbS (green). b) & d) Lorentzian size parameter (Black) and weight % of PbS (Green).

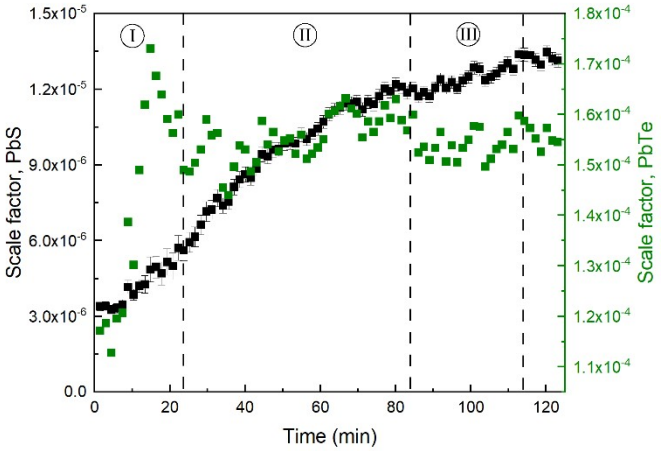

Figure SI 4: Scale factor from Rietveld refinement of $Pb_{0.98}Te_{0.88}S_{0.12}Na_{0.02}$ of both the PbTe matrix phase and the PbS nanostructured phase. The data shows that the scale factor of PbS is increasing, while the scale factor of PbTe is uniform suggesting that there are no evaporating species. The initial increase in scale factor for the PbTe phase is likely due to thermal expansion of the ATOS setup, moving more PbTe into the beam.

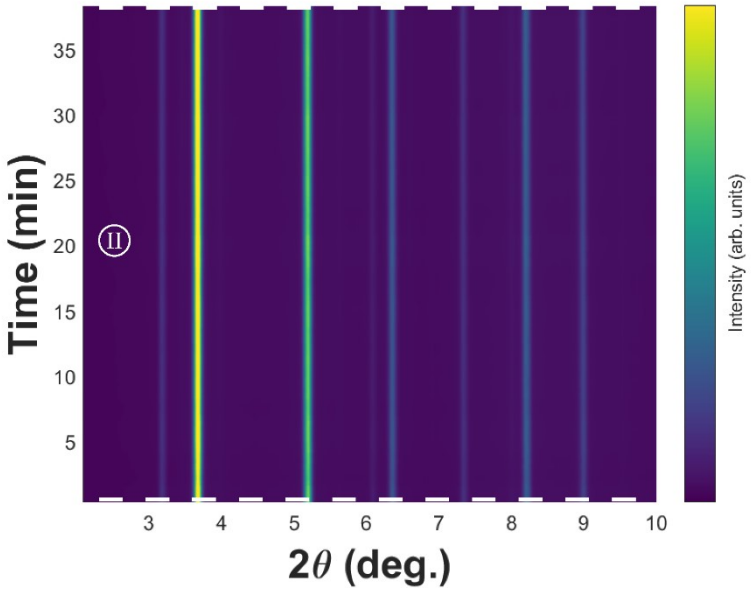

Figure SI 5: Waterfall plot of the diffraction data from the ATOS measurement for $Pb_{0.98}Te_{0.92}S_{0.08}Na_{0.02}$. The data only shows the isotherm region, labeled as II.

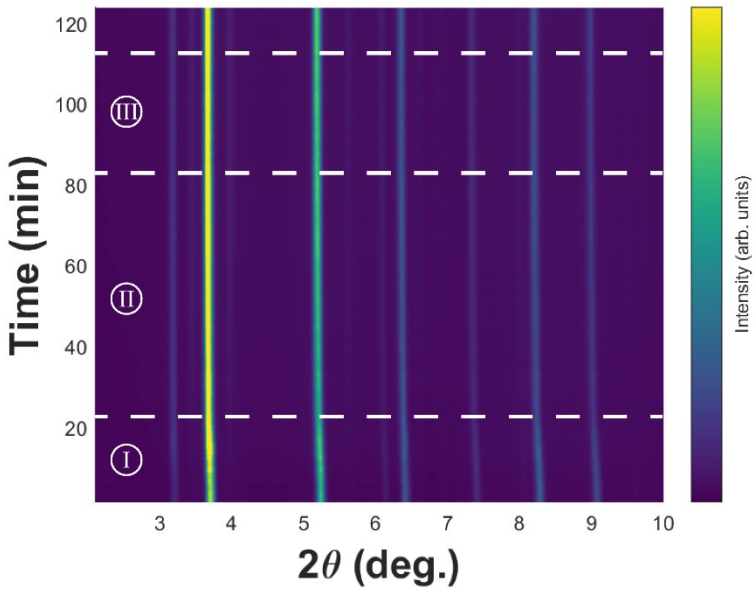

Figure SI 6: Waterfall plot of the diffraction data from the ATOS measurement for $Pb_{0.98}Te_{0.88}S_{0.12}Na_{0.02}$. The data shows the heating (I), isotherm (II) and isotherm + voltage (III) regions, after the isotherm region, the voltage is disconnected, resulting in a slight cooling due to the absence of Joule heating.

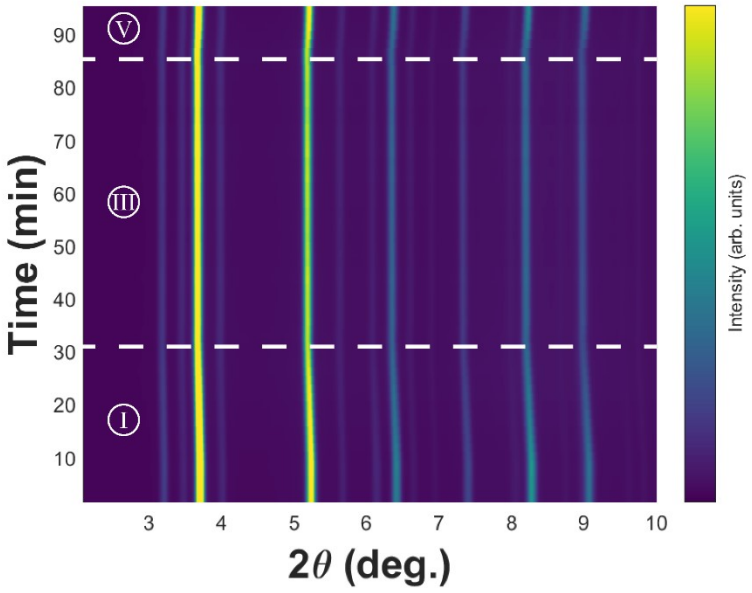

Figure SI 7: Waterfall plot of the diffraction data from the ATOS measurement for $Pb_{0.98}Te_{0.88}S_{0.12}Na_{0.02}$. The data shows the heating (I), isotherm + voltage (III) and cooling (V) regions.

$Pb_{0.98}Te_{1-x}S_x$ – 2 at% Na (x = 0.08 and 0.16)

In both cases, the PbS phase could be refined but both has limitations. In x=0.08, the PbS peaks are weak which results in large uncertainties on the parameters, especially the peak shape parameters which quantifies the size broadening. The unit cell parameters should be correct, as the position of the peak is still easily refinable, even though the peaks are weak. In the x=0.16 case, the peak are much stronger, but also quite narrow. This means that the crystallites are larger, and therefore the analysis regarding size is harder to make, as the size broadening is lower. As such, it is difficult to analyze these cases separately, but they can be used to confirm or refute some of the observations made in the x=0.12 sample. The PbTe phase has a unit cell at room temperature of 6.43024(3) Å and 6.42113(4) Å for the 0.08 and 0.16 sample respectively. Comparing with the 0.12 sample, which is 6.41633(4) Å, this is a clear minima, in accordance with what Girard et. al. observed[2]. The absolute

values are not quite comparable. A plot showing this behavior can be seen in supplementary information Figure SI 2.

The heating and isotherm plateau (Regions I and II in Figure 1) have been applied to both x=0.08 and 0.16, in a similar fashion as 0.12, see Figure SI 3. Both show quite similar behavior to x=0.12. In region (I) the weight fraction of PbS clearly increases prior to reaching the isotherm temperature, confirming that the separation and growth does begin at a lower temperature, at a maximum of 440 °C in 0.16 which is higher than in the 0.12 sample. After the isotherm plateau is reached (Section II), in both samples, the unit cell of the PbS phase stagnates, while the PbTe unit cell continues to increase in a similar fashion as the 0.12 sample. The flattening of the rate seen in 0.12 is not seen in either of these samples, which is likely due to differences in the amount of S incorporated in the PbTe phase and differences in size of the PbS domains. The PbS phase unit cell does not decrease in the x=0.16 phase, whereas it seems to decrease in both the 0.12 and 0.08 phase. Previously, we speculated that the small decrease was either from an excess of Te leaving the PbS phase, or from growth of the crystallites. These results support the latter, as there is no decrease in the 0.16 sample which inherently has larger grains (as seen from Lorentzian size parameters which suggests that $Size_{0.16} > Size_{0.12} \approx Size_{0.08}$) whereas the PbS phase is expected to contain the same amount of Te in all samples. The Lorentzian size parameter has very high uncertainty in both cases, as discussed earlier, but does show a decreasing trend in the isotherm region (B), again similar to the 0.12 sample.

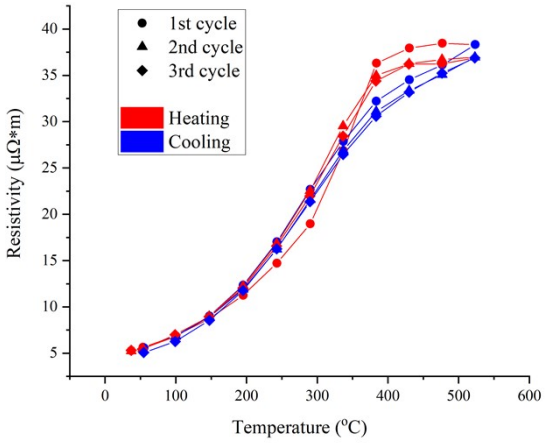

Figure SI 8: First three heating (red) and cooling (Blue) cycles for the $Pb_{0.98}Te_{0.88}S_{0.12}Na_{0.02}$ sample. The shape of the points indicates the cycle number. The first heating is clearly different from the other cycles, suggesting an annealing effect. Additionally, a hysteresis is observed between all heating and cooling cycles. This has not been identified, but is briefly discussed in the main text.

Hysteresis and Na nanostructures in $Pb_{0.98}Te_{0.88}S_{0.12}Na_{0.02}$

The first heating curve is excluded from the main article data, as it shows a clear difference from the subsequent cycles (figure SI 4). This is often seen in samples prepared by pressing and is most likely due to annealing of grain boundary, strain, and other effects induced by the pressing procedure. Additionally, a slight hysteresis between subsequent heating and cooling cycles is observed, especially in the resistivity data, which is very similar to what was previously found in other lead chalcogenide samples. The hysteresis is seen at high temperatures right around the expected temperature for onset of bipolar transport behavior which might suggest that the hysteresis might be coupled to the minority carrier transport properties. This is only conjecture and will require additional exploration. Consequently, only cooling data is shown in the main article.

Wang *et al*.[3] reported change in physical properties of sodium doped PbTe during thermal cycling which was attributed to change in the local sodium environment. This should not affect the conclusions made in the main article for the following reasons. The change reported by Wang et al. was primarily seen in samples with low sodium doping levels (<1.0 at%) where the local sodium environment is expected to be found in the $(Na_{Pb}V_{Te}Na_{Pb})'$-structure as described by Crocker.[4]

Additionally, the change seem by Wang *et al.* was an increase in electrical resistivity and at decrease in thermal conductivity, whereas in this case, the resistivity slightly decreases and the thermal conductivity increases. Therefore, any sodium restructuring should not be the origin of the changes seen in the main text of this article.

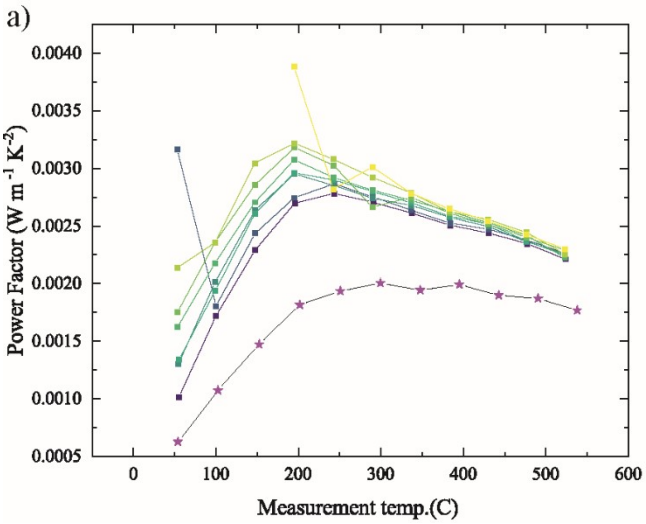

Figure SI 9: High temperature power factor of $Pb_{0.98}Te_{0.88}S_{0.12}Na_{0.02}$ calculated as $\alpha^2\sigma$.

Imaging

Following the nano-/microstructure evolution with PXRD suggested that the PbS nanostructures grows during continuous heating above a certain temperature. To visually confirm the nano-/microstructure of the sample, STEM-EDS was measured on powdered sample prior to SPS pressing the final samples. The result can be seen in Figure SI 10. By examining the STEM images, the x=0.12 shows mostly nanosized domains with a few microsized domains, while the x=0.16 has mostly microsized domains with a few nanosized domains in between. All samples show that even though the sulfur is inhomogeneously distributed throughout the sample, there is a significant amount of sulphur in the PbTe matrix.

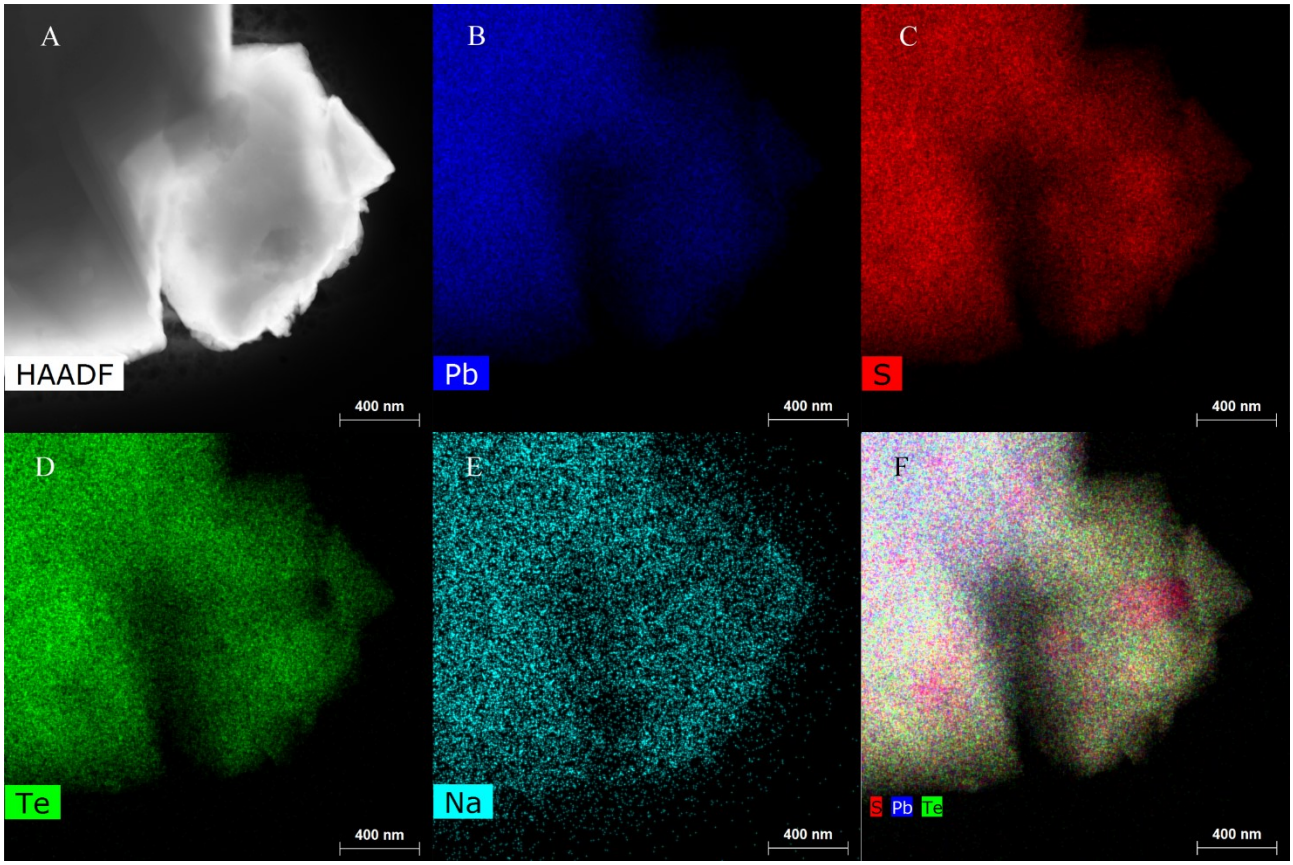

Figure SI 10: STEM-EDX images of $Pb_{0.98}Te_{0.88}S_{0.12}Na_{0.02}$ with elemental resolution. A) HAADF image B) Pb signal C) S signal D) Te signal E) Na signal F) Overlay between S, Te and Pb. It is clear that areas

not containing Te exists, which are the PbS nanostructures.

1 P. Thompson, D. E. Cox and J. B. Hastings, *J. Appl. Crystallogr.*, 1987, **20**, 79–83.

2 S. N. Girard, J. He, X. Zhou, D. Shoemaker, C. M. Jaworski, C. Uher, V. P. Dravid, J. P. Heremans and M. G. Kanatzidis, *J. Am. Chem. Soc.*, 2011, **133**, 16588–16597.

3 X. Wang, I. Veremchuk, M. Bobnar, U. Burkhardt, J.-T. Zhao and Y. Grin, *Chem. Mater.*, 2018, **30**, 1362–1372.

4 A. J. Crocker, *J. Phys. Chem. Solids*, 1967, **28**, 1903–1912.

5 S. I. Sadovnikov, N. S. Kozhevnikova, A. A. Rempel and A. Magerl, *Thin Solid Films*, 2013, **548**, 230–234.